

Study of Reduced Complexity Syndrome Based TTCM Decoder

Hrudia.V.R
M.E Applied Electronics,
ECE Department,
Maharaja Institute of Technology,
Coimbatore – 32, INDIA.,
hrudia.vadakkethil@gmail.com

Sangeetha.P
Assistant professor,
ECE Department,
Maharaja Institute of Technology,
Coimbatore – 32, INDIA.
sangeelaksivam@gmail.com

Abstract

Turbo codes were a major milestone in the forward error correction codes which can even achieve an excellent bit error rates at low SNR. The original proposal was for the BPSK scheme but were soon successful with multilevel coded as well. The “Turbo Trellis Coded Modulation” (TTCM) employing two TCM codes as parallel concatenation of two recursive TCM encoder, and adapted puncturing mechanism to avoid the obvious disadvantage of the rate loss. The iterative decoder of Turbo Trellis Coded Modulation (TTCM) exchanges extrinsic information between the constituent TCM decoders, which imposes a high computational complexity at the receiver. Therefore we conceive the syndrome-based block decoding of TTCM, which is capable of reducing the decoding complexity by disabling the decoder, when syndrome becomes zero. Quantitatively, we demonstrate that a decoding complexity reduction of at least 17% is attained at high SNRs, with at least 20% and 45% reduction in the 5th and 6th iterations, respectively.

Keywords- Block syndrome decoding, TTCM, iterative decoding, BSD BICM.

I. Introduction

In a power-limited environment, the desired system performance should be achieved with the smallest possible transmitted power. The use of error-correcting codes can increase power efficiency by adding extra bits to the transmitted symbol sequence. This procedure requires the modulator to operate at a higher data rate, which requires a wider bandwidth. In a bandwidth-limited environment, the use of higher order modulation schemes can increase efficiency in frequency utilization. In this case, a large signal power would be required to maintain the same system Bit-Error-Rate (BER). In order to achieve improved reliability of a digital transmission system without increasing transmitted power or required bandwidth, both coding and modulation are considered in TCM technology; therefore, TCM is a scheme combining error-correcting coding with modulation. TCM is used for data communication with the purpose of gaining noise immunity over uncoded

transmission without changing the data rate. The use of TCM also improves system without increasing transmitting power and required channel bandwidth. Quadrature Amplitude modulation (QAM) and Quaternary Phase Shift Keying (QPSK) are used in TCM to increase data transmission rate. Since channel bandwidth is a function of the signal-to-noise ratio (SNR), larger signal power would be necessary to maintain the same signal separation and the same error probability if more signals are required to be transmitted without enlarging channel bandwidth.

Trellis coding introduces dependency between every successive transmitting data symbol. The optimum 2-dimensional modulation utilizes the dependency between in-phase and quadrature symbols and the 4-dimensional modulation employs the dependency between symbols of two successive time intervals. Trellis codes and multidimensional modulation are designed to maximize the Euclidean distance between possible sequences of transmitted symbols. Euclidean distance is a straight-line distance between two points in signal constellation. The basic idea of Trellis Coded Modulation is that, instead of sending the symbol ‘m’ formed after the respective modulation is done, an extra parity bit is introduced by doubling the number of constellation points while trying to maintain the same effective throughput.

For example if there are two information bits for 4-level Phase Shift Keying (PSK), a parity bit is being introduced by scaling the original constellation points to eight, i.e. by making it to 8 PSK. As a result the redundant bit can be absorbed by the expanded constellation diagram, instead of increasing the signalling rate of the system (bandwidth). Ungerboeck in his paper fully describes how to employ the TCM schemes in redundant non-binary modulation (symbol based) with the combination of a finite state Forward Error Correction (FEC) encoder, which selects the coded signal sequence. The extra bits formed by corresponding convolution encoder will restrict the possible state transformation among the consecutive phasors to a certain legitimate constellation. The receiver tries to decode the incoming noisy signal by a trellis based soft-decision

maximum-likelihood detector and tries to map it to the each of the legitimate phasor sequence by the restrictions imposed by the convolution encoder.

The term “Trellis” is used to describe this scheme is because the overall operation can be described by a corresponding state transition diagram similar to that of binary convolution encoder. The only difference in TCM is that, here trellis branches are labelled with respect to the redundant non-binary modulated phasors. Since Ungerboeck invented TCM in 1976 and had his papers published in the 1980.s , numerous researches have been working on TCM applications in numerous areas: voice band modems, satellite communications, wireless communications trials, digital subscriber loop, HDTV (high definition television), broadcast channels, CATV (community antenna television) and DBS (direct broadcast satellite) in the 1980.s and 1990.s. Many innovations in TCM technology have been introduced, such as multidimensional TCM (1984-1985), rotationally invariant TCM with M-PSK (1988), TCM with built-in time diversity (1988-1990), TCM with Tomlinson Precoder (1990-1991), TCM with unequal error protection (1990), multilevel coding with TCM (1992-1993), and concatenated coding with TCM (1993-present).

TTCM constitutes a bandwidth-efficient near-capacity joint modulation/coding solution, which relies on the classic turbo coding architecture, but involves the bandwidth-efficient Trellis Coded Modulation (TCM) instead of the constituent convolutional codes. More explicitly, the constituent TCM codes, which can be optimally designed using Extrinsic Information Transfer (EXIT) charts, are concatenated in a parallel fashion and iterative decoding is invoked at the receiver for exchanging extrinsic information between the pair of TCM decoders. In order to reduce its decoding complexity, we propose to reduce the effective number of decoding iterations by appropriately adapting the syndrome based block decoding approach of, for TTCM. The main focus of this project is to study and compare the performance of conventional TTCM decoder and syndrome based TTCM decoder schemes with the uncoded QPSK using Gray mapping scheme.

II .The Existing System

TTCM Decoder is much similar to that of binary turbo codes, except the difference in the nature of the information passed from one decoder to other decoder respectively and the treatment of the very first decoding step and schematic of the decoder is shown in the Here, the main concern is how the symbol-based non binary TTCM scheme is being done. In symbol-based non binary scheme the systematic bit as well as the parity bits are transmitted together as in the form of complex enveloped symbol and cannot be separated from the extrinsic components, since the noise and the fading that effect the parity components will also affects the corresponding

systematic components.

Disadvantages:

1. Increased hardware complexity.
2. Increased computational complexity.

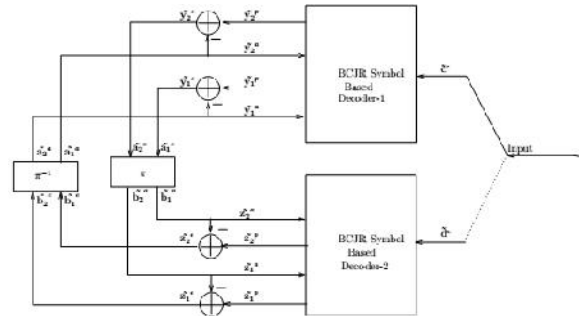


Fig. 1 Existing TTCM Decoder

Therefore, here in this case the symbol-based information can be split into two components:

1. the a-priori component of the non binary symbol provided by the alternative decoders.
2. the inseparable extrinsic information as well as the systematic components of the nonbinary symbol.

Now, we can concentrate the working of the TTCM decoder. The received symbols are separated into two different symbol to make sure that upper decoder receives only the symbols encoded by the upper encoder vice versa for the second decoder as well and this can be described as the first step in the decoding. After this, each decoder produces its symbol based probabilities and generates the a-priori and extrinsic information based on Log-Based BCJR algorithms. The decoders then provides the corresponding a posteriori (\tilde{y}^p, \tilde{z}^p) which is subtracted with incoming a-priori (\tilde{a}^a, \tilde{b}^a) information to make sure that each of the decoder doesn't receive the same information more than once. The extrinsic information are then interleaved/deinterleaved by the random interleavers to become the a-priori information and made to iterate between them. During the final decoding the a posteriori information are deinterleaved from the decoder-2 and uses the Hard decision for selecting the maximum a-posteriori probability associated with the information word.

III. Block Based Syndrome Decoder For Ttcm

In order to quantify the reduction in decoding complexity using the proposed BSD-TTCM, we can analyze the performance of the 8-state TTCM for 8PSK transmissions over an AWGN channel. We have to first heuristically determine the optimum design parameter L_{min} while ensuring that the BSD-TTCM yields the same BER as the conventional TTCM decoder. We can also benchmark the performance of our proposed BSDTTCM decoder against the conventional hard-decision aided high-SNR Early Termination (ET) criterion.

The comparison of the BER performance of the proposed BSD-TTCM to that of the classic TTCM decoder is need to be done and quantify the complexity reductions achieved in terms of the number of effective decoding iterations as well as the percentage of non-decoded blocks at each iteration.

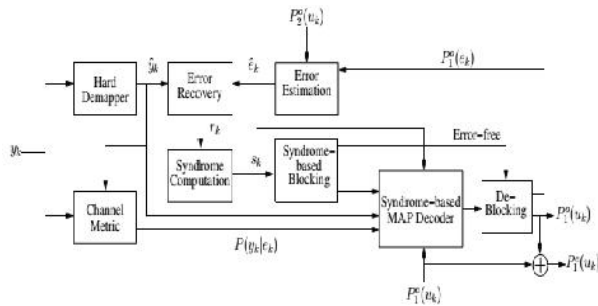


Fig.2 Block Based Syndrome Decoder

In order to reduce its decoding complexity, we propose to reduce the effective number of decoding iterations by appropriately adapting the syndrome based block decoding approach for TTCM. In contrast to the trellis of the conventional convolutional decoder which uses the Generator Matrix (GM), G, for generating its trellis, the trellis used for syndrome decoding is based on the syndrome former HT. The idea of syndrome decoding was first conceived in for the efficient hard decoding of convolutional codes using an error trellis¹. Later, soft-decision syndrome decoding approaches were presented. Which were based on the error and codeword trellis, respectively. In the error trellis of a syndrome decoder, the state probabilities are a function of the channel errors rather than of the coded sequence. Consequently, at high SNRs, the syndrome decoder is more likely to encounter a zero state due to the predominant error-free transmissions.

This underlying property of syndrome decoding has been exploited in for developing a Block Syndrome Decoder (BSD) for convolution codes, which divides the received sequence into erroneous and error-free parts based on the syndrome. More specifically, the BSD only decodes the erroneous blocks, with the initial and final states of the trellis initialized to zero. Therefore, the decoding complexity is substantially reduced at higher SNRs. This approach was then further extended to turbo codes, where a pre-correction sequence was also computed at each iteration to correct the errors. Thus, the decoding complexity was reduced not only at higher SNRs, but also for the higher-indexed iterations. Furthermore, a syndrome-based MAP decoder was proposed in for designing an adaptive low complexity decoding approach for turbo equalization.

In schematic of the proposed BSD-TTCM Decoder, Only one constituent decoder is shown here. Like in the conventional TTCM decoder, both constituent

decoders have a similar structure and iterative decoding is invoked for exchanging extrinsic information between the two. P_a , P_e and P_o are the a-priori, extrinsic and a-posteriori probabilities related to the i^{th} decoder; e_k is the channel error on the transmitted symbol and u_k is the information part of e_k .

Figure above shows the schematic of one of the two constituent decoders of our proposed Block Syndrome Decoder conceived for TTCM (BSD-TTCM). The received symbol sequence y_k is demapped onto the nearest point x_i in the corresponding 2^n -ary constellation diagram, yielding the hard-demapped symbols \hat{y}_k , i.e.

$$\hat{y}_k = \text{argmin}(y_k - x_i), \quad (1)$$

for $i \in \{0, \dots, 2^n - 1\}$ and,

$$y_k = x_k + n_k. \quad (2)$$

Here, x_k is the complex-valued phasor corresponding to the n -bit transmitted codeword c_k , which is obtained using the $2n$ -PSK mapper μ as follows:

$$x_k = \mu(c_k) \quad (3)$$

and n_k is the noise experienced by the k the symbol in an AWGN channel.

In TTCM, the odd and even symbols are punctured for the upper and lower TCM decoders respectively, while the parity bits of the corresponding hard-demapped symbols are set to zero. Then, a pre-correction sequence \hat{e}_k , which is predicted by the error estimation module, is used for correcting any predicted errors. This sequence is initialized to zero for the first iteration. The syndrome s is computed for the corrected symbol stream r using the syndrome former HT as follows:

$$s = rH^T, \quad (4)$$

where, the j^{th} bit of r is r_k related to that of \hat{y}_k and \hat{e}_k , for $k \in \{0, \dots, n-1\}$, as follows:

$$r_{k,j} = \hat{y}_{k,j} \oplus \hat{e}_{k,j}, \quad (5)$$

with $r_k = [r_{k,0}, \dots, r_{k,j}, \dots, r_{k,n}]$, $\hat{y}_k = [\hat{y}_{k,0}, \dots, \hat{y}_{k,j}, \dots, \hat{y}_{k,n}]$, and $\hat{e}_k = [\hat{e}_{k,0}, \dots, \hat{e}_{k,j}, \dots, \hat{e}_{k,n}]$.

Then the syndrome is analyzed for sake of dividing the received block into error-free and erroneous sub-blocks. The error-free sub-blocks are then subjected to a hard-decision and only the erroneous sub-blocks are passed to the MAP decoder. Like in the conventional TTCM decoder, both constituent decoders have a similar structure and iterative decoding is invoked for exchanging extrinsic information between the two.

A. Syndrome-Based Map Decoder

Invoked the syndrome-based MAP decoder in the proposed BSD-TTCM of Figure. In contrast to the conventional MAP decoder, which operates on the basis of

the codeword trellis, its syndrome-based MAP counterpart relies on the error trellis constructed using the syndrome former H^T . More explicitly, each trellis path of a codeword trellis represents a legitimate codeword. By contrast, each path of an error trellis specifies the hypothetical error sequence causing a departure from a specific legitimate codeword trellis path. Furthermore, both trellises have the same complexity and every error path in the error trellis uniquely corresponds to a codeword path in the codeword trellis. The classic MAP algorithm computes the A-Posteriori Probability (APP) $P^o(u_k)$ for every M-ary transmitted information symbol u_k given by $P^o(u_k) = P(u_k = m | y)$ for $m \in \{0, 1, \dots, M-1\}$, Where $M = 2^{n-1}$, $(n-1)$ is the number of bits in an information symbol and $R = (n-1)/n$ is the coding rate. However, the syndrome-based MAP computes the APP for every M-ary channel error experienced by the information symbol. In other words, u_k is the transmitted information symbol in the codeword trellis, whereas, it is the M-ary channel error experienced by the information symbol in the error trellis. Therefore, the channel information $P(y_k | x_k)$ for the transmitted codeword x_k , is modified to $P(y_k | e_k)$ for the channel error e_k , which is formulated as:

$$P(y_k | e_k) = \frac{1}{2\pi\sigma^2} \cdot e^{-\frac{|y_k - \hat{x}_k|^2}{2\sigma^2}}$$

Where σ^2 is the noise variance per dimension and \hat{x}_k is given by:

$$x_k = \mu(\hat{c}_k), \quad (7)$$

for

$$\hat{c}_{k,j} = \hat{y}_{k,j} \oplus e_{k,j} \quad (8)$$

Here, we have $\hat{c}_k = [\hat{c}_{k,0}, \dots, \hat{c}_{k,j}, \dots, \hat{c}_{k,n}]$ and

$$e_k = [e_{k,0}, \dots, e_{k,j}, \dots, e_{k,n}].$$

The APP of u_k can be calculated in terms of the forward-backward recursive coefficients α_k and β_k as follows:

$$P^o(u_k) = \sum_{\substack{(\hat{\tau}, \tau) \Rightarrow \\ u_k = m}} \gamma_k(\hat{\tau}, \tau) \cdot \alpha_{k-1}(\hat{\tau}) \cdot \beta_k(\tau)$$

where the summation implies adding all the probabilities associated with those transitions of the error trellis for which $u_k = m$. Furthermore, we have:

$$\begin{aligned} \gamma_k(\hat{\tau}, \tau) &= P^a(u_k) \cdot P(y_k | e_k), \\ \alpha_k(\tau) &= \sum_{\text{all } \hat{\tau}} \gamma_k(\hat{\tau}, \tau) \cdot \alpha_{k-1}(\hat{\tau}), \\ \beta_{k-1}(\hat{\tau}) &= \sum_{\text{all } \tau} \gamma_k(\hat{\tau}, \tau) \cdot \beta_k(\tau), \end{aligned}$$

Where $P^a(u_k)$ is the a-priori probability of the information part of the error e_k , i.e. u_k . At the first iteration, no a-priori information is available; hence, it is initialized to be equiprobable, i.e. $P^a(u_k) = 1/M$.

B. Error Estimation

Similar to the bit-wise pre-correction sequence proposed for turbo codes, we make an estimate of the 2n-ary symbol error in each iteration to ensure that the Hamming weight of the syndrome decreases with ongoing iterations. While the extrinsic information was used in for the estimating the pre-correction sequence, we have improved the estimation by using the APP. This proceeds as follows:

- The information part of the pre-correction sequence \hat{e}_k is set to the hard decision of the APP of the information symbol ($P^o(u_k)$) computed by the other decoder.
- The parity part of \hat{e}_k is set to the hard decision value of the APP of the codeword ($P^o(e_k)$) gleaned from the previous iteration of the same decoder, which yields the same information symbol as that computed in the first step.

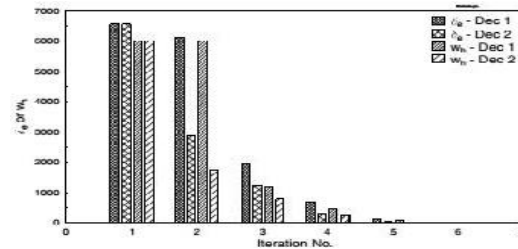


Fig.3 Variation in the number of differences (δ_e) between the actual and estimated error.

Figure 3 verifies the accuracy of our pre-correction sequence. Here the average number of differences δ_e , between the actual and estimated error, is plotted against the number of iterations at an SNR per bit of $E_b/N_0 = 3.8$ dB, for 1000 frames of 12000 TTCM-8PSK symbols transmitted over an AWGN channel. Both constituent decoders are characterized separately, which are referred to as Dec 1 and Dec 2 in Figure 5.13. Observe that the differences decrease at each successive iteration, eventually reaching zero at the 6th iteration. Furthermore, the Hamming weight w_h of the syndrome closely follows the same trend.

C. Syndrome-Based Blocking

The Hamming weight of the syndrome sequence of Eq. (4) decreases at higher SNRs, since only a few errors are encountered. It also decreases with each successive iteration as seen in Fig. 2. This is because the errors are estimated at each iteration and the corresponding correction is applied to the received symbols. In other words, upon increasing the number of iterations or SNR, the syndrome exhibits longer sequences of zeros, which indicates error-free transmission. This fact can be exploited to partition the received block into error-free and erroneous segments. This is achieved by heuristically choosing a design parameter, $L_{\min} = (L_{\text{start}} + L_{\text{end}} + 1)$, which is the minimum number of consecutive

SNR RANGE	L_{min}
$E_b/N_0 \leq 3.5\text{dB}$	51
$E_b/N_0 = 3.6\text{dB}$	111
$E_b/N_0 = 3.7\text{dB}$	401
$E_b/N_0 = 3.8\text{dB}$	3001
$E_b/N_0 = 3.9\text{dB}$	5001

zero syndromes after which the subblock is deemed to be error-free. Furthermore, L_{start} L_{end} define the start and end of the next and previous sub-blocks, respectively. If L_0 is the length of the subblock having at least L_{min} consecutive zero syndromes, then the initial $L_{end} = (L_{min}-1)/2$ symbols of this sub-block are appended to the previous erroneous block and the last $L_{start} = (L_{min}-1)/2$ symbols are appended to the following erroneous block. Only the remaining $(L_0-L_{min}+1)$ symbols are considered error-free. This ensures that the trellis of the erroneous sub-blocks starts from and terminates at the zero state. The hypothetical error-free blocks do not undergo further decoding and the corresponding APPs of the error-free trellis segment are set to 1. On the other hand, the erroneous blocks are fed to a MAP decoder with the initial and final states of the decoding trellis set to zero.

The design parameter L_{min} strikes a trade-off between the BER performance attained and the complexity imposed. A lower value of L_{min} will result in more error-free blocks, thereby reducing the complexity imposed. However, it will degrade the BER performance of the system. On the other hand, a higher value of L_{min} will give a better BER performance but at the expense of an increased decoding complexity.

IV. Results And Discussions

In order to quantify the reduction in decoding complexity achieved using the proposed BSD-TTCM, we have analyzed the performance of the 8-state TTCM for 8PSK transmissions over an AWGN channel. Furthermore, a block length of 512 TTCM-8PSK symbols and 8 iterations were used. We have first heuristically determined the optimum design parameter L_{min} while ensuring that the BSD-TTCM yields the same BER as the conventional TTCM decoder. Since the Hamming weight of the syndrome decreases with the SNR, the optimum L_{min} has to increase with the SNR to ensure that the performance is not compromised. We have particularly focused our attention on the high-SNR region (i.e. $E_b/N_0 \geq 3.5$) and the L_{min} value was appropriately optimized for every 0.1dB increment in E_b/N_0 , as listed in Table I.

Table I. Optimum L_{min} For Varying E_b/N_0 .

It must be mentioned here that the optimum L_{min} for a particular value of E_b/N_0 will depend on the code parameters as well as on the channel type. The BER performance of the BSD-TTCM is compared to that of the conventional TTCM decoder in Figure 4.

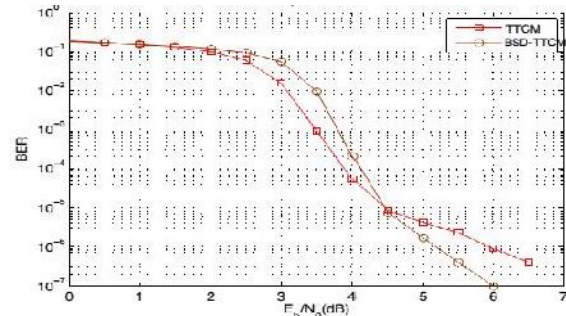


Fig.4 BER performance curve of BSD-TTCM and conventional TTCM decoding.

The BER performance of both BSD-TTCM and conventional TTCM decoder for various interleaver lengths are shown in figure 5 and figure 6.

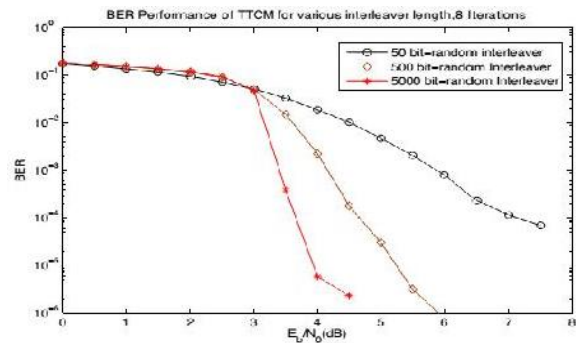


Fig.5 BER performance of TTCM for various interleaver length.

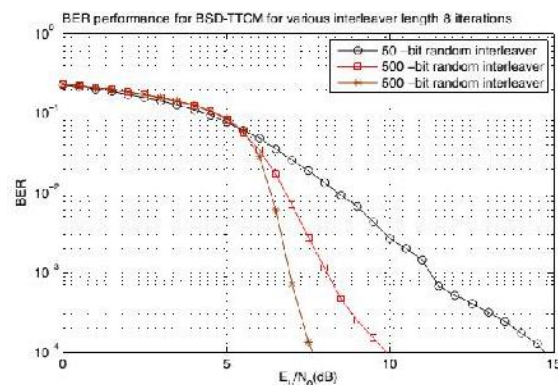


Fig.6 BER performance of BSD TTCM for various interleaver

length.

The BER performance of BSD-TTCM based on the design parameter L_{min} of Table I is compared to that of the conventional TTCM decoder in Figure 7.

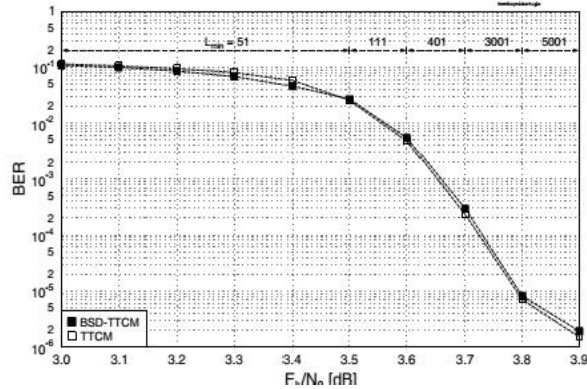


Fig.7 BER performance curve of BSD-TTCM based on L_{min} .

In figure 7 it can be seen that both decoding schemes exhibit a similar performance. The corresponding reduction in the decoding complexity is quantified in Figure 8 in terms of:

- Equivalent number of iterations (Right axis): Each iteration is weighted by the percentage of the symbols that had to be decoded, which quantified the equivalent (or effective) number of iterations.
- Percentage of No-Decoding (Left axis): This quantifies the total number of symbols in the error-free sub-blocks as a percentage of the frame length (i.e. 512).

In Figure 5.18, as E_b/N_0 is increased from 3.0dB to 3.5dB for $L_{min} = 51$, the number of effective iterations is reduced to a minimum of 4.8 at 3.5dB. This is equivalent to a $(100 \times (6 - 4.8) / 6) = 20\%$ reduction in the number of decoding iterations. Furthermore, the percentage of non-decoded symbols for each iteration also increases, reaching a maximum of 45% for the 6th iteration at 3.5dB. Then, when L_{min} is increased to 111 at 3.6dB, the number of equivalent iterations increases to 5. This corresponds to a reduction of $(100 \times (6 - 5) / 6) \approx 17\%$ compared to the maximum of 6 iterations and it is therefore still significant. Moreover, the percentage of non-decoded symbols in iterations 2 to 5 decreases, while that in the 6th increases. This is because at this point there are two counter-acting forces:

- 1) An increased L_{min} would reduce the number of error free blocks.
- 2) An increased E_b/N_0 would decrease the Hamming weight of the syndrome sequence and, therefore, increase the number of error-free blocks.

A similar trend is observed, when E_b/N_0 is increased further. Hence, the proposed scheme reduces the effective number of iterations by at least one, i.e. by 17%, for high SNRs. Furthermore, at least a 20% complexity reduction is achieved for the 5th iteration and 45% for the 6th iteration.

And also benchmarked the performance of the proposed BSDTTCM decoder against the conventional hard-decision aided high-SNR Early Termination (ET) criterion in Figure 7. The proposed scheme outperforms ET by at least 0.5 iteration at high SNRs.

A. EXIT charts analysis

Extrinsic Information Transfer (EXIT) chart analysis is powerful that is used to check the convergence of the iterated decoders. BER chart is one of most powerful tool to analysis the performance how good the decoder is, but it was not able to explain in detail how the decoder converges when an iterative decoding is done. EXIT chart measures the Mutual Information (MI) that is exchanged between the constituent decoder in a iterative process. The EXIT chart is expressed in terms of the Log Likelihood ratio of both apriori information I_a and extrinsic information I_e .

The extrinsic iterative decoding trajectory that are connected through the interleavers, the extrinsic outputs of the demapper becomes the a priori information to the decoders and the extrinsic output of the decoder become the a priori inputs to demapper. This exchange of the extrinsic information is what is known to be Extrinsic information transfer chart (EXIT chart) and can be plotted into a single diagram by combining both the demapper and decoder transfer characteristics.

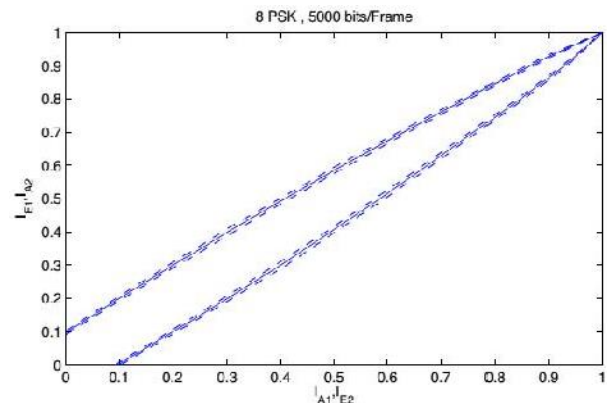


Fig.8 EXIT Chart for TTCM 8PSK, 5000 bits/frame.

B. EXIT band charts

EXIT band chart describes the generalised mutual information transfer characteristic and the probabilistic convergence behaviour of the iterative decoding. The mutual information between the information bit and the corresponding extrinsic information are obtained in the same manner how the EXIT charts are calculated. The difference between the EXIT band chart and EXIT chart is that here the simulation are kept running for various channel realisation and the interleavers used here. Thus we can obtain the various mutual information of the output extrinsic information from the constituent decoders. Then, for each E_b/N_0 we can represent the output extrinsic information as the average extrinsic information ($avg(I_e)$) and

as $(\text{avg}(I_E \pm \text{std } I_E))$

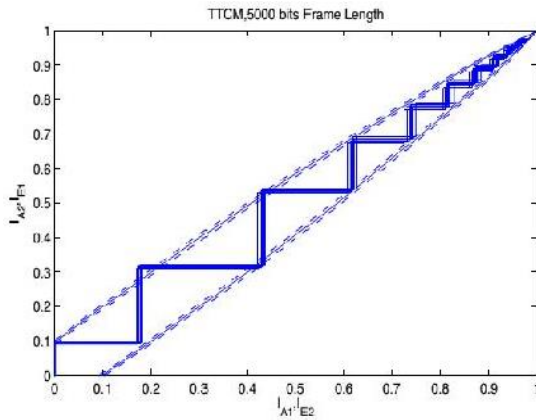


Fig.9 Mutual Information trajectories and EXIT band chart of TCM.

The obtained EXIT band chart with the trajectories can be illustrated in the Figure 9. The width of the std deviation curve depends on the information frame length, as Frame length increases the EXIT band chart shrink to the ordinary EXIT charts.

C. Comparative study of BSD - TCM and BSD- BICM schemes

Another coded modulation scheme distinguishing itself by utilizing bit-based interleaving in conjunction with Gray signal constellation labeling is referred to as Bit-Interleaved Coded Modulation (BICM). More explicitly, BICM combines conventional convolutional codes with several independent bit interleavers, in order to increase the achievable diversity order. With the aid of bit interleavers the code's diversity order can be increased to the binary Hamming distance of a code. The number of parallel bit-interleavers equals the number of coded bits in a symbol for the BICM scheme proposed in. The performance of BICM is better than that of TCM over uncorrelated (or perfectly interleaved) narrowband Rayleigh fading channels, but worse than that of TCM in Gaussian channels due to the reduced Euclidean distance of the bit-interleaved scheme.

Recently iterative joint decoding and demodulation assisted BICM referred to as BICM-ID was proposed in, which uses SP based signal labeling. The approach of BICM-ID is to increase the Euclidean distance of BICM and hence to exploit the full advantage of bit interleaving with the aid of soft-decision feedback based iterative decoding.

The BICM considers trellis-coded modulation using bit interleaving and iterative decoding with hard decision feedback. The scheme not only achieves a performance gain over existing TCM schemes, but also provides a common framework for TCM over channels with a wide variety of fading statistics. In addition, the system

allows an efficient combination of punctured convolutional codes and multiphase/level modulation, and therefore offers a simple mechanism for variable-rate transmission. The paper begins with a short description of the relevant TCM literature, to emphasize the foundations of the suggested scheme.

A known pitfall of BICM is the reduced free Euclidean distance caused by the "random modulation" inherent in a bit-interleaved scheme. This results in performance degradation over conventional TCM for AWGN channels. Likewise, when the fading is slow and the interleaving insufficient, conventional TCM can outperform BICM. The performance of BICM can be improved by iterative decoding (ID) using hard decision feedback. In particular, BICM-ID converts a 2^M -ary signaling channel to M parallel binary channels. With proper bit labeling, a large binary Hamming distance between coded bits can be indirectly translated into a large Euclidean distance.

Figure 10 shows the block diagram of BICM-ID. Due to the weak coupling between the code and modulation in BICM-ID, a variety of binary convolutional codes and modulation methods can be flexibly combined. Also, convolutional codes punctured from a single mother code can be used to enhance flexibility. For simplicity, the discussion below focuses on a rate-2/3 code and 8PSK modulation.

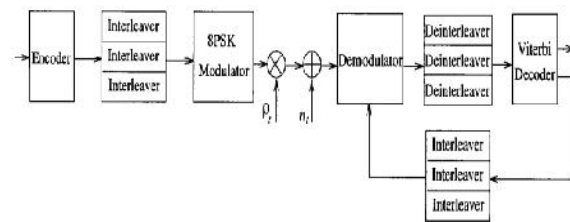


Fig.10 Block diagram of BICM-ID

Input information bits are first encoded by a convolutional encoder. Then, a bit-by-bit interleaver permutes the order of encoder output bits. Note that the interleaver is composed of three independent bit interleavers corresponding to the three bit positions in an 8PSK symbol. The interleaved bits are grouped into modulation symbols. The purpose of bit-by-bit interleaving is, first, to break the correlation of sequential fading coefficients, and to maximize the diversity order of the system. Second, it removes the correlation among the sequentially coded bits, as well as the bits associated with the same channel symbol. This is important in reducing error propagation in the iterative decoding. Finally, the standard Viterbi algorithm is used at decoding. Since BICM is bit oriented, the decoding for punctured codes is straightforward - if a bit is punctured at the encoder, the associated bit metrics are taken as zero at the decoder.

Here implemented the decoder for BICM using BSD instead of the conventional Viterbi or logmap

decoder. And then compared the performance of BICM-BSD with TTCM-BSD in terms of BER.

The following section studies the performance of BSD-TTCM and BSD BICM-ID, using computer simulations. The complexity of the coded modulation schemes is compared in terms of the number of decoding states and the number of decoding iterations. For a TCM or BICM code of memory M , the corresponding complexity is proportional to the number of decoding states $S=2^M$. Since TTCM schemes invoke two component TCM codes, a TTCM code invoking t iterations and using an S -state component code exhibits a complexity proportional to $2.t.S$ or $t.2^{M+1}$.

As for BICM ID schemes, only one decoder is used but the demodulator is invoked in each decoding iteration. However, the complexity of the demodulator is assumed to be in significant compared to that of the decoder. Hence, a BICM-ID code with t iterations using an S -state code exhibits a complexity proportional to $t.S$ or $t.2^M$.

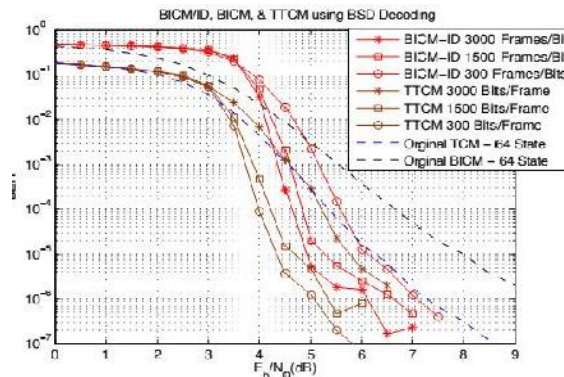


Fig.11 BICM-ID and TTCM using BSD Decoding

Figure shows the effects of the decoding complexity on the BSD TTCM and BSD BICM-ID schemes performance in the context of an 8PSK scheme over AWGN channels using a block length of 4000 IBs (2000 symbols). The 64-state TCM, 64-state BICM, 8-state TTCM using four iterations and 16-state BICM-ID along with four iterations exhibit a similar complexity. At a BER of 10^{-4} , TTCM requires about 0.6dB lower SNR than BICM-ID, 1.6dB less energy than TCM and 2.5dB lower SNR than BICM. When the coding complexity is reduced such that 8-state codes are used in the TCM, BICM and BICM-ID schemes, their corresponding performance becomes worse than that of the 64-state codes, as shown in Figure. In order to be able to compare the associated performance with that of 8-state BICM-ID using four iterations, 8-state TTCM along with two iterations is employed. Observe that due to the insufficient number of iterations, TTCM exhibits only marginal advantage over BICM-ID.

V. Conclusions

The proposed BSD-TTCM only decodes the blocks deemed to be erroneous, which are identified using the syndrome sequence. Therefore, the decoding complexity

is reduced. More specifically, at least 20% and 45% complexity reduction was achieved for the 5th and 6th iterations, respectively. Furthermore, a pre-correction sequence is estimated at each iteration for reducing the decoding complexity of the forthcoming iterations. Comparison of the BER performance of the proposed BSD-TTCM to that of the classic TCM decoder can be done and quantified the complexity reductions achieved in terms of the number of effective decoding iterations as well as the percentage of non-decoded blocks at each iteration. EXIT charts can be used to analyze the mutual information exchange between the iterative decoders. At a given complexity TCM performs better than BICM in AWGN channels, but worse in uncorrelated narrow band Rayleigh fading channels. However, BICM-ID using soft decision feedback outperforms TCM and BICM over both AWGN and uncorrelated narrowband Rayleigh fading channels at the same decoding complexity. TTCM has shown superior performance over the other coded modulation schemes studied, but exhibited a higher error floor due to the uncoded IBs over uncorrelated narrowband Rayleigh fading channels. BICM-ID outperforms conventional TCM over Rayleigh fading channels, and compares favorably with TCM over AWGN channels. BICM-ID provides a simple mechanism for variable-rate transmission. Its features, attractive in software radios, are also suitable for hybrid approaches using ASIC's or FPGA's.

VI. Acknowledgements

The author would like to thank the Department of Electronics and Communication Engineering, MIT, Coimbatore for providing laboratory facilities and opportunity for experimental setup.

VII. References

- [1] Bahl .L , Cocke J., Jelinek. F, and Raviv.J(1974) 'Optimal decoding of linear codes for minimizing symbol error rate (corresp.)', IEEE Trans. Inf. Theory, vol. 20, no.2, pp.284-287.
- [2] Cavers J, and Ho P (1992) 'Analysis of error performance of trellis coded modulation in rayleigh – fading', IEEE Transaction on Communication, vol.40 pp. 74-83.
- [3] Geldmacher J, Hueske K , and Gotze J 'Syndrome based block decoding of convolutional codes' in Proc. 2008 IEEE International Symposium on Wireless Communication Systems, pp. 542-546.
- [4] NG S. X (2002) 'Coded modulation schemes for wireless channels' Ph.D. Dissertation, Department of Electronics and Computer Science, University of Southampton
- [5] Paaske E (1974) 'Short binary convolutional codes with maximal free distance for rates 2/3 and 3/4', IEEE Transaction on Information Theory vol. IT-29, pp. 683-689.

- [6] Robertson and Worz (1998) ' Bandwidth-efficient turbo trellis-coded modulation using punctured component codes', IEEE J. Sel. Areas Commun.,vol. 16, no. 2, pp. 206-218.
- [7] Schalkwijk J and Vinck A (1975) 'Syndrome decoding of convolutional codes' IEEE Trans. Commun., vol. 23, no. 7, pp. 789-792.
- [8] Ten Brink S (2001) 'Convergence behaviour of iteratively decoded parallel concatenated codes', IEEE Transactions on Communications, vol. 49, no. 10, pp. 1727-1737.
- [9] Ungerboeck G (1982) 'Channel coding with multilevel/phase signals', IEEE Trans. Inf. Theory, vol. 28, no. 1, pp.55-67.
- [10] Zehavi E (1992) '8-psk trellis codes for rayleigh fading channel', IEEE Transaction On Communication, vol. 40, pp. 873-883.
- [11] Zunaira Babar,Soon Xin Ng and Lajos Hanzo (2013)'Reduced-Complexity Syndrome-Based TTCM Decoding ', IEEE communications letters, vol. 17, no. 6, pp. 1220- 1223.